CUSP DYNAMICS AND IONOSPHERIC OUTFLOW

S.A. FUSELIER[1], S.B. MENDE[2], T.E. MOORE[3], H.U. FREY[2], S.M. PETRINEC[1], E.S. CLAFLIN[1] and M.R. COLLIER[3]
[1]*Lockheed Martin Advanced Technology Center*
[2]*University of California, Berkeley*
[3]*Goddard Space Flight Center*

Abstract. One of the IMAGE mission science goals is to understand the dayside auroral oval and its dynamic relationship to the magnetosphere. Two ways the auroral oval is dynamically coupled to the magnetosphere are through the injection of magnetosheath plasma into the magnetospheric cusps and through the ejection of ionospheric plasma into the magnetosphere. The ionospheric footpoints of the Earth's magnetospheric cusps are relatively narrow regions in invariant latitude that map magnetically to the magnetopause. Monitoring the cusp reveals two important aspects of magnetic reconnection at the magnetopause. Continuous cusp observations reveal the relative contributions of quasi-steady versus impulsive reconnection to the overall transfer of mass, energy, and momentum across the magnetopause. The location of the cusp is used to determine where magnetic reconnection is occurring on the magnetopause. Of particular interest is the distinction between anti-parallel reconnection, where the magnetosheath and magnetospheric field lines are strictly anti-parallel, and component merging, where the magnetosheath and magnetospheric field lines have one component that is anti-parallel. IMAGE observations suggest that quasi-steady, anti-parallel reconnection is occurring in regions at the dayside magnetopause. However, it is difficult to rule out additional component reconnection using these observations.
The ionospheric footpoint of the cusp is also a region of relatively intense ionospheric outflow. Since outflow also occurs in other regions of the auroral oval, one of the long-standing problems has been to determine the relative contributions of the cusp/cleft and the rest of the auroral oval to the overall ionospheric ion content in the Earth's magnetosphere. While the nature of ionospheric outflow has made it difficult to resolve this long-standing problem, the new neutral atom images from IMAGE have provided important evidence that ionospheric outflow is strongly controlled by solar wind input, is 'prompt' in response to changes in the solar wind, and may have very narrow and distinct pitch angle structures and charge exchange altitudes.

1. Introduction

When the IMAGE mission was conceived more than seven years ago, the major science objectives included understanding the dayside auroral oval and its dynamic relationship to the Earth's magnetosphere and magnetopause. The investigation of the dayside auroral oval was driven by two important results from in situ measurements of the auroral zone and the Earth's magnetopause. The first result was that there exist direct connections between the magnetopause and the dayside auroral ovals through the Earth's magnetospheric cusps. The second result was that ionospheric ion outflow occurs from the dayside auroral oval.

Space Science Reviews **109:** 285–312, 2003.

Two imaging sensors on the IMAGE spacecraft make unique contributions to the study of the dayside auroral oval and its relationship to the magnetosphere and magnetopause. One of these sensors is a photon imager and the other is a neutral atom imager. The Spectrographic Imager (SI) is one of the photon imagers on the spacecraft (Mende *et al.*, 2000). This imager uses a series of slits and a grating to make images in the far ultraviolet in 2 fairly narrow wavelength bands. One of the wavelength bands uses the slit arrangement to eliminate the non-Doppler shifted Lyman Alpha produced by the Earth's geocoronal hydrogen and image Doppler shifted Lyman Alpha produced by protons that undergo charge exchange and de-excitation in the Earth's upper atmosphere. This wavelength channel of the SI (called SI12) has produced the first global images of aurora created by proton precipitation (Mende *et al.*, 2001). The other SI imager, called SI13, is not discussed here. In addition to the unambiguous determination of proton precipitation, the SI12 has another advantage over FUV imagers that observe LBH or other wavelengths associated primarily with electron precipitation into the auroral zone. Quantitative measure of the dayside aurora from these other imagers requires subtraction of a substantial dayglow background. In contrast, the dayglow background in the SI12 imager is negligible (Mende *et al.*, 2000). The SI12 image cadence is set by the 2 min spacecraft spin rate, with one image (accumulated over a 10 s period) produced every 2 min.

The Low Energy Neutral Atom (LENA) imager is one of three neutral atom imagers on the spacecraft (Moore *et al.*, 2000). This imager uses a tungsten surface to convert a fraction of low energy neutral atoms into negative ions. The negative ions are then accelerated in an electrostatic field and passed through a time-of-flight mass spectrometer. The arrival direction of the neutral atom is preserved in this analysis and the mass spectrometer allows distinction between hydrogen and oxygen. The energy range of the imager (for directly converted neutrals) is the same as that for ionospheric outflow (from a few eV to several hundred eV). Thus, the LENA imager provides the first global imaging of ionospheric outflow by imaging the neutrals created from charge exchange of ionospheric ion outflow with the Earth's upper atmosphere and hydrogen geocorona (Moore *et al.*, 2001).

This paper reviews some of the unique contributions to the understanding of the dynamic relationship between the dayside auroral oval and the magnetosphere and magnetopause from the SI12 and LENA imagers. The paper is divided into two major sections. The first major section reviews the observations of the footpoint of the magnetospheric cusp in the northern hemisphere and its relationship to the Earth's magnetopause. Within this section are sub-sections discussing cusp observations under conditions of northward interplanetary magnetic field (IMF), under conditions when the IMF rotates from north to south, and under conditions of southward IMF. The second major section reviews the observations of ionospheric ion outflow and its relationship to the auroral zone in general and the cusp footpoint in particular.

2. The Earth's Magnetospheric Cusps

Cusps exist in the Earth's magnetosphere because, ideally, there must be two points at northern and southern high latitudes where the Earth's magnetic field lines converge. In a completely closed magnetopause (i.e., a magnetopause where there is no magnetic reconnection between magnetospheric and magnetosheath field lines), the magnetic field lines that skim the magnetopause all map to this single cusp point. Magnetic reconnection modifies this simple picture at the magnetopause and causes the footpoint of the cusp to increase in size. However, even for an open magnetopause, the cusp is expected to be a fairly narrow region in longitude and, especially, in latitude (e.g., Newell and Meng, 1992).

Around the time the cusp was discovered, it was believed to be a region where shocked solar wind plasma in the magnetosheath had direct access to the ionosphere. Indeed, for a completely closed magnetopause, there is still a narrow region stretching from the cusp footpoint out through the magnetopause where the field strength is very low. The discovery of a narrow cusp, where plasma with magnetosheath energies was precipitating and the magnetic field strength was low (Heikkila and Winningham, 1971; Frank, 1971; Russell *et al.*, 1971) appeared to support this view of the cusp.

An alternate view of the cusp developed with the realization that magnetic reconnection was occurring at the Earth's magnetopause (e.g., Rosenbauer *et al.*, 1975; Reiff *et al.*, 1977). In this view, the cusp footpoint is still the site of precipitating magnetosheath plasma, but the entry point and characteristics of the precipitation depends on the external magnetic field in the magnetosheath. With the identification of clear evidence of magnetic reconnection at the Earth's magnetopause in the late 1970's and early 1980's (e.g., Sonnerup *et al.*, 1981), it became important to understand how the cusp precipitation could be interpreted in terms of this reconnection process.

The properties of the precipitating ion and electron populations in the cusp were put on firm observational grounds by setting specific definitions for the energy and flux (e.g., Newell and Meng, 1988, 1992). By fixing the definition, statistical studies of the cusp were able to demonstrate that the cusp moved in latitude and longitude in response to the IMF orientation. In addition to a dipole tilt effect (Zhou *et al.*, 2000), the cusp migrates from high magnetic latitude ($\sim$80°) to lower latitudes ($\sim$70°–75°) as the IMF Bz component changes from positive to negative (Burch *et al.*, 1973; Carbary and Meng, 1988; Zhou *et al.*, 2000; Wing *et al.*, 2001). Also, in the northern hemisphere, the cusp is located at post-noon magnetic local times when the IMF has a duskward component (+By) and is located at pre-noon magnetic local times when the IMF has a dawnward component (−By) (Candidi *et al.*, 1989; Newell *et al.*, 1989; Zhou *et al.*, 2000). Finally, it was shown that there is often a velocity dispersion observed in the cusp precipitation. For northward IMF, this dispersion is such that the highest energies of the precipitating ions are observed at the most poleward edge of the cusp (e.g., Woch and Lundin, 1992)

and, for southward IMF, the dispersion is reversed such that the highest energies are observed at the most equatorward edge of the cusp (e.g., Reiff *et al.*, 1977). This velocity dispersion, and the pitch angle variations contained within it (Burch *et al.*, 1986), proved to be a key element in linking precipitation in the cusp with magnetic reconnection at the magnetopause.

The above features of the cusp, determined largely from statistical study of the precipitation, are readily explained by magnetic reconnection at the magnetopause. The location of the cusp moves from high to low latitude as the IMF turns from northward to southward because reconnection favors the magnetopause at high latitudes for northward IMF and the magnetopause at lower latitudes for southward IMF, where dayside magnetospheric field lines are eroded away (e.g., Zhou *et al.*, 2000). The longitudinal control of the cusp location requires a more detailed explanation of magnetic reconnection at the magnetopause (discussed below). The velocity dispersion is a direct result of the finite extent of the reconnection neutral line at the magnetopause and the convection of the reconnected magnetic field lines in the magnetosphere. For northward IMF, reconnected field lines are pulled sunward and the highest energy ions, entering the magnetosphere near the reconnection neutral line, precipitate at the poleward edge of the cusp at high latitudes. Lower energy ions precipitate equatorward of this high latitude edge because they take longer to travel from the magnetopause to low altitudes, and, as they travel along the reconnected field line, the field line convects sunward. Eventually, the sunward convection slows and the field lines convect around the flanks of the magnetopause.

When the IMF is southward, the field line convection is poleward (and tailward) instead of sunward. Thus, the highest energy ions precipitate at the equatorial edge of the cusp at 'low' latitudes. Using known features of magnetic reconnection at the magnetopause and a relatively simple magnetospheric model, this velocity dispersion and other detailed features of the ion precipitation in the cusp for southward IMF have been reproduced (e.g., Onsager *et al.*, 1993).

Despite significant progress in understanding cusp precipitation, there are several questions about the cusps and their relationship to the magnetopause and magnetic reconnection that remain unanswered. In general terms, in situ measurements have been unable to conclusively determine when and where magnetic reconnection occurs at the magnetopause.

Statistical analysis of cusp observations appears to indicate that magnetic reconnection is a quasi-steady process that probably does not cease for long periods of time (e.g., Newell and Sibeck, 1993). In contrast, individual passes through the cusp and ground based observations have been interpreted as evidence that cusp precipitation could occur by short pulses of reconnection of the order of a few minutes long separated by longer periods where the reconnection is not occurring (e.g., Smith and Lockwood, 1990). In situ observations at the magnetopause do not resolve this controversy. These observations indicate that magnetic reconnection is common and, during multiple passes through the magnetopause, appears to be

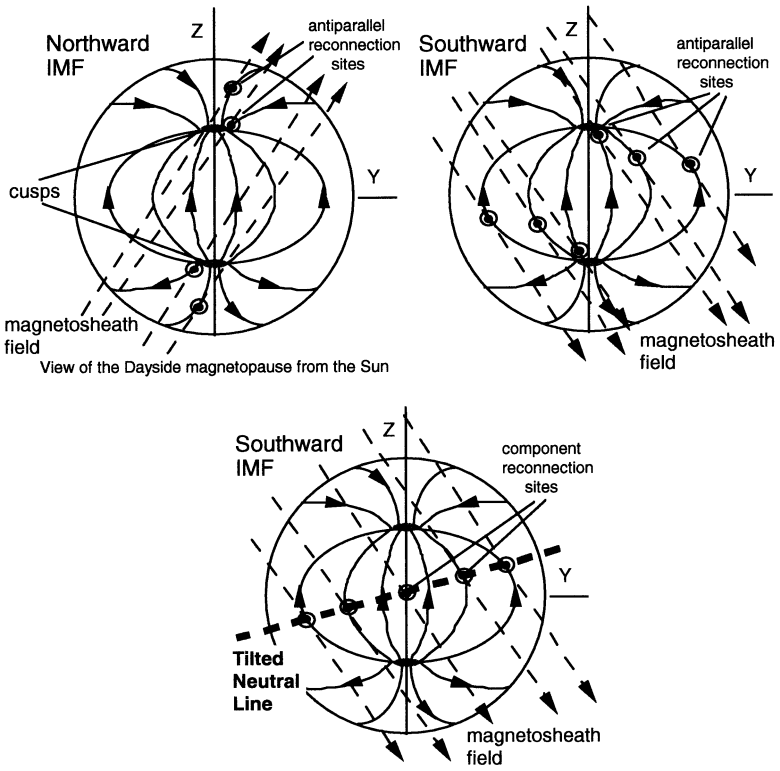

Figure 1. Reconnection sites for northward and southward IMF. The view is from the sun and the dashed lines are magnetosheath field lines and the solid lines are magnetospheric field lines. The first two panels show how the anti-parallel reconnection model predicts high latitude reconnection sites (poleward of the magnetospheric cusps) when the IMF is northward and lower latitude reconnection sites (equatorward of the cusps) when it is southward. The differences between this model and the tilted neutral line (component reconnection) model (third panel) are most evident in the subsolar region.

'quasi-steady' (e.g., Phan *et al.*, 2000). However, there is always the ambiguity that spacecraft remain in the reconnection layer for short periods of time ($\sim$ minutes) and the observational techniques used to demonstrate that reconnection is occurring do not address the reconnection rate.

Another shortcoming of in situ measurements of reconnection at the magnetopause is that they give only qualitative information on the location of the reconnection neutral line. This ambiguity concerning where reconnection is occurring has resulted in two different models for the process. In the first model, reconnection is assumed to occur only in those regions where the magnetosheath field lines draped against the magnetopause are nearly anti-parallel to the magnetospheric field lines at the magnetopause (e.g., Crooker, 1979). This assumption nicely explains that reconnection occurs at high latitudes when the IMF is northward and lower latitudes when the IMF is southward. The explanation is illustrated in the left and middle

panels of Figure 1. These panels show the magnetospheric magnetic field lines at the magnetopause as viewed from the sun. Anti-parallel reconnection sites occur at high latitudes poleward of the cusp when the magnetosheath magnetic field has a northward component. Anti-parallel reconnection sites occur at lower latitudes equatorward of the cusp when the magnetosheath magnetic field has a southward component.

A second model assumes that, when the IMF is northward, reconnection occurs at high latitudes (as in the anti-parallel reconnection model). However, when the IMF is southward, it is assumed that reconnection occurs along a line that passes through the subsolar point and has a tilt that depends on the IMF By component (e.g., Sonnerup *et al.*, 1974). This 'tilted neutral line model' assumes that reconnection is driven in the subsolar region by the dynamic pressure of the shocked solar wind, so that strictly anti-parallel magnetic fields are not a necessary condition. Thus, in the subsolar region for southward IMF, only one component of the magnetosheath and magnetospheric field lines needs to be anti-parallel. This type of reconnection is referred to as component reconnection and is illustrated in the right hand panel of Figure 1. Some in situ observations at the magnetopause for southward as well as northward IMF suggest that component reconnection is occurring (Gosling *et al.*, 1990; Fuselier *et al.*, 1997).

The IMAGE observations of proton precipitation in the cusp provide a new perspective on the 'when' and 'where' of magnetic reconnection. Quasi-continuous monitoring of the cusp proton precipitation allows distinction between pulsating, intermittent reconnection and a quasi-steady cusp. The global imaging of the cusp footpoint (with essentially no dayglow background) may allow distinction between anti-parallel and component (tilted neutral line) reconnection models.

In the next three sections, the cusp under conditions of northward IMF, northward to southward rotations of the IMF, and southward IMF are discussed. In each section, the 'when' and 'where' of magnetic reconnection are discussed in terms of pulsating or quasi-steady reconnection and component or anti-parallel reconnection.

3. The Cusp for Northward IMF

Under conditions of northward IMF, the footprint of the cusp in the IMAGE SI12 data is observed to be a bright spot located poleward of the auroral oval (Frey *et al.*, 2002; Fuselier *et al.*, 2002a). Figure 2 shows examples of the cusp spot observed on 18 September 2000. In each frame, the aurora is shown in magnetic latitude – magnetic local time (MLT) with local noon at the top and dawn to the right (i.e., from the vantage point above the north magnetic pole). The spot is located at magnetic latitude between 70° and 80° and near noon MLT in each of the frames. The three frames are not in time order. Rather, they demonstrate that the spot can

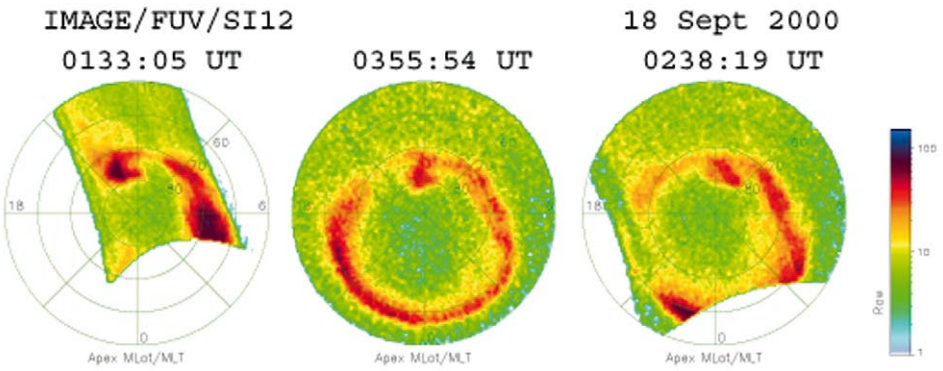

Figure 2. Cusp aurora observations during a period of prolonged northward IMF. In each panel, the cusp aurora emissions are the highly localized spot located poleward of the cusp at about 78° latitude. The spot is observed continuously (the images are selected from over 180 consecutive images) and changes location in local time as IMF By changes sign.

be located post-noon (left hand panel), very nearly at noon (middle panel), and pre-noon (right hand panel).

Figure 2 illustrates three properties of the cusp footpoint for northward IMF that warrant further discussion. These three properties are the persistence of the cusp aurora emissions, the localization of the emissions into a fairly narrow spot, and the motion of the spot. The first property is related to the persistence and steadiness of magnetic reconnection at the magnetopause and the other two properties are related to the location of reconnection at the magnetopause.

The cusp aurora spots in the three panels in Figure 2 have similar intensities because the solar wind dynamic pressure during this period was relatively constant. In general, the intensity of the cusp aurora has been shown to depend on solar wind dynamic pressure (Frey *et al.*, 2002). This correlation should not be surprising. Higher solar wind dynamic pressures occur when the solar wind density and/or the velocity are high and these conditions result in correspondingly higher flux of relatively high-energy protons precipitating in the cusp.

The non-linear response of the SI12 imager to proton energy enhances the dynamic pressure effect. The imager detects Doppler-shifted Lyman Alpha produced by protons that have precipitated in the upper atmosphere, charge exchanged to neutral H, and emitted Lyman Alpha. Non-Doppler shifted Lyman Alpha (at $\sim$121.6 nm) is eliminated in the imager because the Earth's geocorona at about 121.6 nm is much more intense than the proton aurora. The imager has 0.2 nm resolution and the center of the first wavelength band is at 121.8 nm. When considering proton flux and the subsequent Lyman Alpha production in the image, the maximum response of the SI12 imager comes from 2–3 keV protons (Gerard *et al.*, 2001). Lower (and higher) energy protons produce correspondingly smaller signal in the SI12 imager. The variation in the sensitivity is non-linear so that, for protons with incident energy of $\sim$1 keV, the transmission is about 50% of the peak

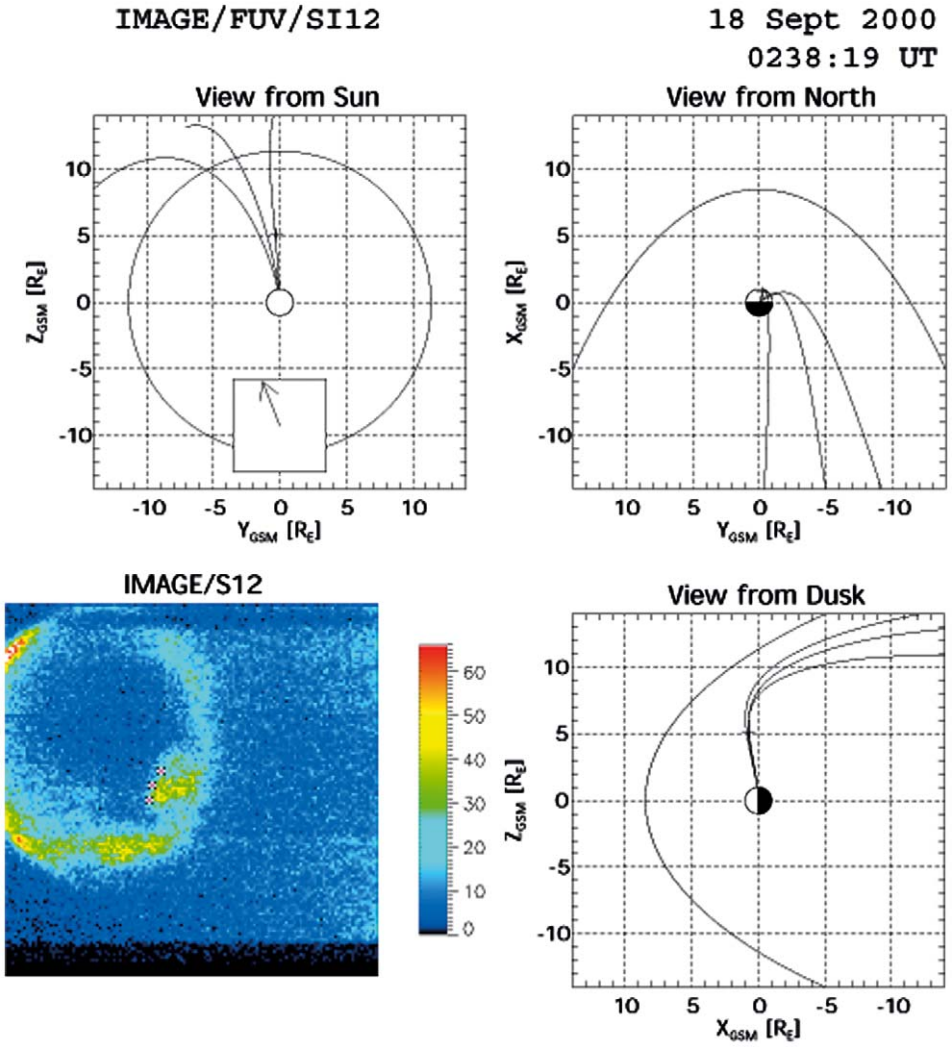

Figure 3. Field line mapping of cusp aurora. The lower left hand panel shows the raw FUV/SI12 image. Three pixels (identified by the black/white/red checkerboard patterns) are mapped to the magnetopause using a magnetospheric magnetic field model. The cusp aurora spot maps to a narrow region on the magnetopause that is located poleward of the cusp. This region is located on the same side of the magnetopause as the draped magnetosheath magnetic field lines (the IMF clock angle is shown in the view from the sun projection in the upper left hand panel).

at 2–3 keV, and for protons with incident energy of ∼500 eV, the transmission is about 10% of the peak (Gerard *et al.*, 2000). The response to relatively high-energy protons has important implications for observing cusp precipitation and its relationship to solar wind dynamic pressure. Solar wind protons under average solar wind conditions have characteristic energies of about 1 keV. However, the shocked solar wind proton distribution in the magnetosheath has a significant proton population

(∼20% or more) above ∼1 keV (e.g., Gosling and Robson, 1985). The proton flux above 1 keV depends on the two solar wind quantities that make up the dynamic pressure, the velocity (higher velocity results in a higher flux of protons above 1 keV) and the density (more protons in the solar wind results in a higher flux of protons above 1 keV in the magnetosheath).

Accounting for the non-linear response of the SI12 imager to the proton precipitation is important in considering the persistence of the cusp aurora. For nominal solar wind dynamic pressures (∼1.5 nPa), the cusp aurora is not detected. However, when dynamic pressures are above about 5 times the nominal solar wind dynamic pressure, cusp aurora is observed. This is also true for the Spectrographic Imager 13 and Wideband Imaging Camera on the IMAGE spacecraft that detect a combination of proton and electron precipitation. Normally, the electron precipitation has much more energy flux than the proton precipitation. However, during periods of high solar wind dynamic pressure, the cusp proton precipitation is so intense that it produces detectable signal at 135.6 nm and at LBH wavelengths between 140 and 160 nm (e.g., Frey *et al.*, 2002). Although not identified as proton precipitation, intense cusp emissions have been observed by other FUV imagers that observe in LBH wavelengths (e.g., Milan *et al.*, 2000).

Frey *et al.* (2002) showed that the cusp footpoint is present continuously during extended periods of northward IMF and high solar wind dynamic pressure. The three frames in Figure 2 are representative of the more than 180 consecutive images of the cusp aurora spot that were observed during a period that extended over 6 hours. These observations indicate that magnetic reconnection at the magnetopause can be a very steady process. Although the reconnection rate is not determined from these observations, the consistency of the cusp footpoint demonstrates that rate does not decrease to zero for any significant length of time.

The localization of the cusp footpoint and its motion are the result of the nature of magnetic reconnection at the magnetopause (Fuselier *et al.*, 2002a). The footpoint is highly localized because the reconnection neutral line occupies a relatively narrow region of the magnetopause. The footpoint moves in magnetic local time because the neutral line at the magnetopause moves with changes in the IMF By component.

Figure 3 shows three perspective views of the tracing of the magnetic field lines that originate from the poleward edge of the cusp footpoint observed at 0238:19 UT (the right hand panel in Figure 2). The lower left hand panel in Figure 3 shows the raw image from the SI12 imager (i.e., not mapped into the MLT-magnetic latitude coordinate system as in the left hand panel in Figure 2). The black and white, 3×3 checkerboard patterns at the poleward edge of the cusp aurora spot in Figure 3 show the origins of the field line tracings for the three field lines in the perspective views surrounding the image. These checkerboard patterns also demonstrate that the cusp aurora spot is well resolved by the SI12 imager. The diameter of the complete spot is approximately 12–15 pixels in the image (or ∼1000 km in the ionosphere at ∼100 km altitude).

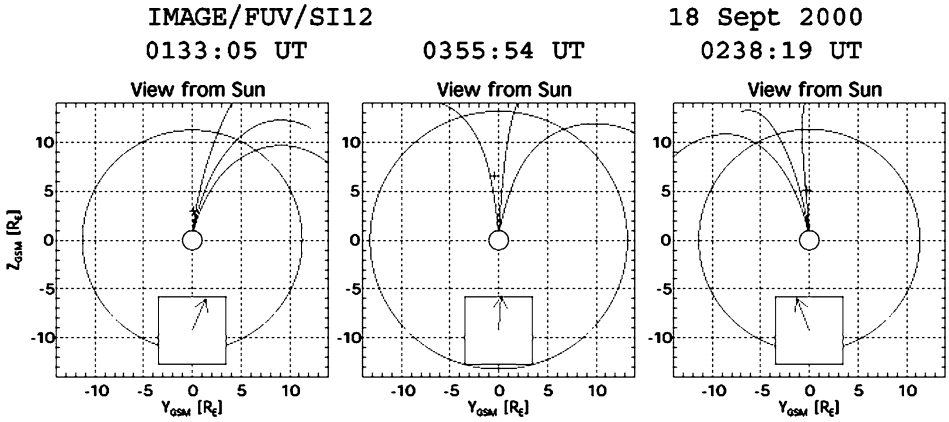

Figure 4. View from the sun projections of the cusp footpoint field line mapping for the three images in Figure 2. The region on the magnetopause where the reconnection neutral line is located follows the changes in the IMF By component. This indicates that the reconnection neutral line is located where the magnetospheric and draped magnetosheath field lines are most nearly anti-parallel.

The three field lines were traced in the Tsyganenko magnetic field model (Tsyganenko, 1995) assuming that the emissions occurred at ∼100 km altitude in the ionosphere. These field lines are lobe field lines that, in the absence of reconnection, originate deep in the Earth's magnetotail, skim the magnetopause along its high latitude boundary (in the view from the duskside, they appear to be further inside the magnetosphere), and become the poleward part of the cusp field lines down to low altitudes. When the IMF is northward, these lobe field lines will reconnect with draped magnetosheath field lines, forming an open field line that exits the magnetopause at high latitudes. Magnetosheath protons will have direct access to the ionosphere along these open field lines. The orientation of the draped magnetosheath field lines depends on the IMF By component. In the inset box in the upper left hand panel in Figure 3, the IMF clock angle (convected from the upstream solar wind monitor position to the magnetopause using the solar wind speed) is shown. Since magnetospheric magnetic field lines originate in the southern hemisphere, the northern hemisphere lobe field lines that form the poleward edge of the cusp aurora are most nearly anti-parallel to the draped magnetosheath field lines. Thus, the reconnection neutral line (where the lobe and magnetosheath field lines interconnect) occupies a fairly narrow region of the magnetopause where the magnetosheath and lobe field lines are most nearly anti-parallel.

Figure 4 shows how the field line tracings from the cusp aurora in Figure 2 depend on the IMF clock angle. The three panels each show three field lines traced from the poleward edge of the cusp aurora spots in Figure 2. The perspective view in Figure 4 is from the sun, looking along the sun-Earth line and the box inset in each panel shows the IMF clock angle. It is evident that the locations of the lobe field lines that map from the cusp change with IMF clock angle. When the

IMF By component is positive (left hand panel of Figure 4), the lobe field lines participating in reconnection are located on the duskside of the magnetopause and the cusp aurora spot is also on the duskside (left hand panel of Figure 2). When the IMF By component is nearly zero (middle panel of Figure 4), reconnection occurs near local noon and the cusp aurora spot is near local noon (middle panel of Figure 2). When the IMF component is negative (right hand panel of Figure 4), reconnection occurs on the dawnside and the cusp aurora spot is also on the dawnside (right hand panel of Figure 2).

From the northward IMF observations in Figures 2 through 4, the following features of magnetic reconnection are evident. First, reconnection can be very steady, occurring continuously over periods lasting many hours (Frey *et al.*, 2002). Second, the reconnection neutral line is reasonably localized and associated with the region where the high latitude lobe field lines in the magnetosphere are nearly anti-parallel to the draped magnetic field lines in the magnetosheath (Fuselier *et al.*, 2002a). The reconnection neutral line follows changes in IMF By so that only those magnetospheric field lines that are most nearly anti-parallel to the draped magnetosheath field lines participate in reconnection. The effect of changing the IMF By is readily evident in the longitudinal motion of the cusp (Frey *et al.*, 2002). These features of the cusp location strongly favor anti-parallel reconnection. However, as discussed in the next two sections, the images do not necessarily rule out component reconnection.

4. The Cusp for IMF Rotations from North to South

In the previous section, it was demonstrated that the cusp footpoint was localized when the IMF was northward. Observations in Figure 5 show how the cusp footpoint changes character and location as the IMF rotates from north to south. Changes in the orientation of the IMF are rarely smooth. However, the IMF rotation from north to south was relatively smooth during the sequence of images shown in Figure 5. The inset in each image shows the clock angle of the solar wind magnetic field (convected to the magnetopause and to the ionosphere using the solar wind velocity). The view is from the Earth (i.e., the opposite vantage point that is shown in Figure 4). Thus, in Figure 5, positive (negative) By appears on the left (right) hand quadrant.

Starting with the first image in the upper left hand corner of Figure 5, the IMF was northward and had only a small (positive) By component. The cusp footpoint is the distinct bright spot at 12 MLT, nearly 85° latitude, and poleward of the auroral oval. This spot persists as long as the IMF has a strong northward component. As the IMF rotates southward (starting with the fifth image in the sequence), the cusp footpoint moves in the equatorward and pre-noon MLT direction, and eventually merges with the pre-noon auroral oval. There is another distinct change in the auroral oval evident in the last three images in Figure 5. As the IMF component turns

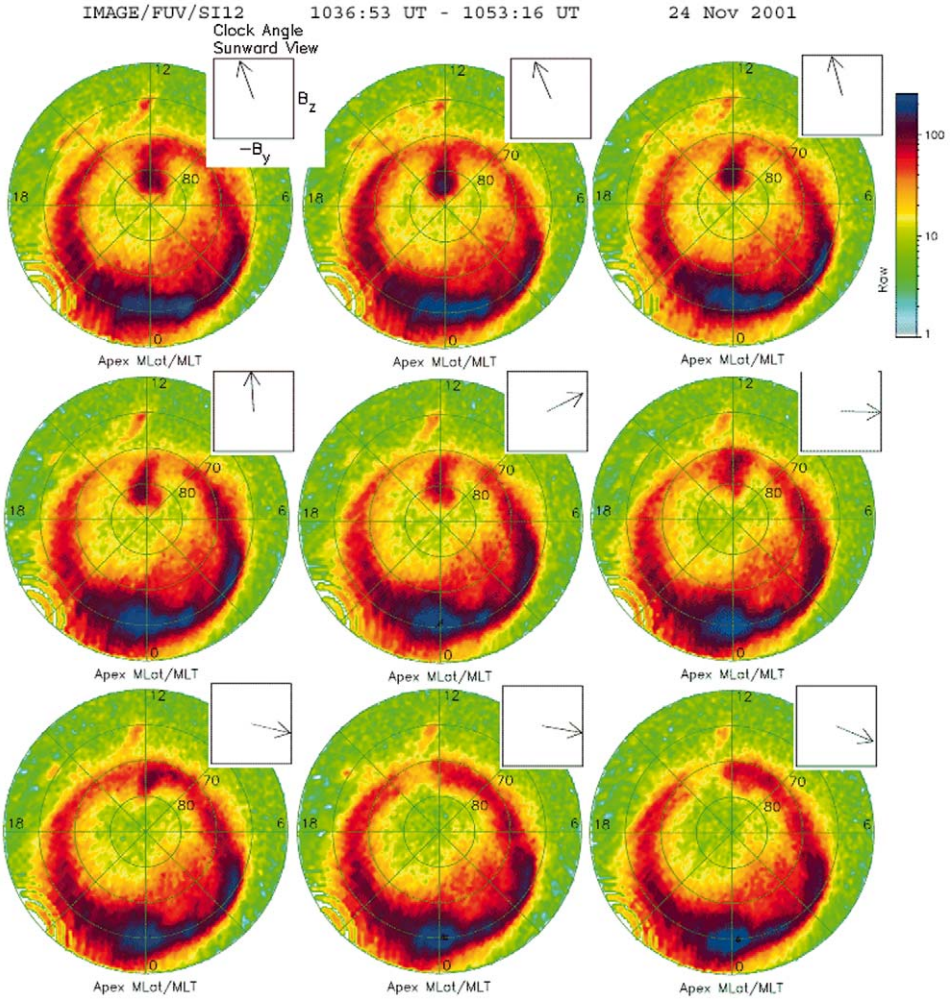

Figure 5. Changes in the cusp footpoint as the IMF rotates from north to south. In this sequence of images (each image is acquired in 10 s and successive images are 2 min apart), the cusp footpoint moves t lower latitudes from its position poleward of the auroral oval as the IMF rotates. When the IMF has a southward component, the cusp footpoint is merged with the auroral oval but there is a gap in the emissions between 12 and 15 MLT.

southward, a break develops in the auroral oval between 12 and 15 MLT so that, at the end of the transition, there are significantly more auroral emissions on the dawnside (i.e., the same side as the IMF) than on the duskside. The MLT changes in the auroral oval will be discussed in the next section.

Figure 6 (adopted from Crooker *et al.*, (1979)) shows how a rotation of the neutral line from high latitudes to lower latitudes can explain the motion of the cusp footpoint as the IMF rotates from north to south. Shown is the view of the magnetopause from the sun. The dashed lines show the orientation of the IMF

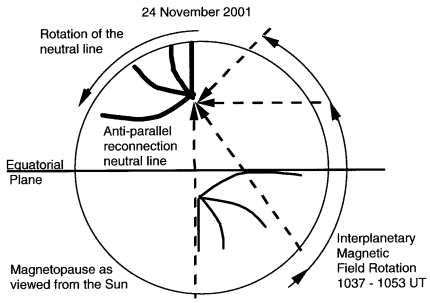

Figure 6. Illustration of how the anti-parallel reconnection neutral line rotates about the cusp as the IMF rotates from north to south. As the IMF rotates, the neutral lines, initially located poleward of the cusps, rotate to positions such that magnetic field lines equatorward of the cusps are reconnecting (see also Figure 1). Thus, the cusp footpoint moves equatorward as the IMF rotates.

as it rotates from a purely northward orientation to an orientation with southward and dawnward components. The solid lines show how the reconnection neutral line (assuming anti-parallel reconnection at the magnetopause) rotates from high to lower latitudes. The pivot points of these neutral lines are the northern and southern cusps. Because the event in Figure 6 occurred during northern hemisphere winter, the northern cusp was located at higher latitudes above the equatorial plane than the southern cusp.

As the neutral line rotates, magnetic field lines equatorward of the cusp start participating in reconnection. These field lines map to lower latitudes in the ionosphere than the high latitude field lines poleward of the cusp. Thus, as the neutral line rotates to lower latitudes, the footpoint of the cusp also moves to lower latitudes.

From the observations in Figure 5 and the interpretation in Figure 6, the following features of reconnection are evident. First, as the IMF rotates from north to south, reconnection does not stop and restart. The cusp aurora spot seen poleward of the auroral oval during the northward IMF interval moves equatorward and spreads out over the oval on the pre-noon side as the IMF rotates southward. This equatorial motion indicates that the reconnection site changes from high latitudes to low latitudes as the IMF rotates. The anti-parallel reconnection model provides one interpretation of the change in the reconnection site as the IMF rotates. Hinged about the northern cusp location, the neutral line at high latitude rotates to lower latitudes so that the reconnection switches from lobe field lines (that cross the equatorial plane in the Earth's magnetotail) to dayside magnetospheric field lines (that cross the equatorial plane on the dayside). A similar rotation occurs for the neutral line hinged at the southern cusp. Second, the cusp emissions are one-sided when the IMF rotates southward. By the time the IMF has a southward component, the cusp emissions are located at the same latitude as the auroral oval and are on the pre-noon side of the auroral oval. There is a clear gap between 12 and 15 MLT, with cusp aurora is located on the same side as the IMF By component. The next

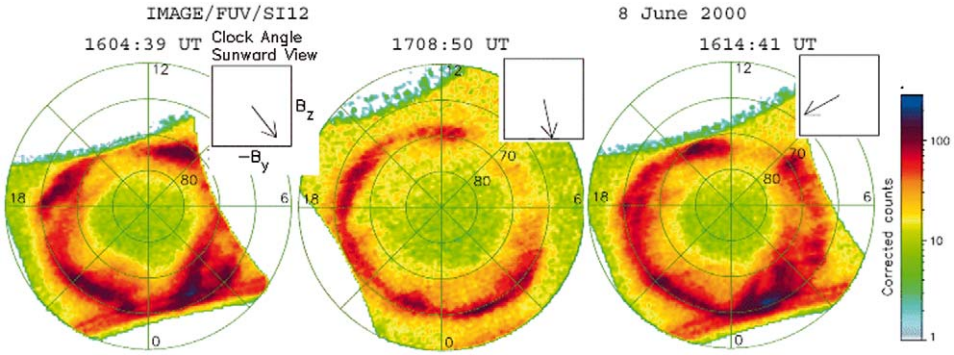

Figure 7. Three images during a southward IMF interval showing that the cusp footpoint moves as the IMF By changes. The clock angles are shown as viewed from the Earth. The cusp is located on the dawnside (duskside) of the auroral oval when the IMF By is negative (positive).

section describes in more detail how the cusp aurora changes with IMF By when the IMF Bz component is negative.

5. The Cusp for Southward IMF

Figure 7 shows three images of the aurora taken during a period when the IMF was persistently southward. Similar to Figure 2, the images in Figure 7 are not in time sequence. Rather, they represent three different IMF By values during the period when the Bz component was negative. When the IMF By component is negative (left hand panel), the cusp aurora emissions are located on the pre-noon side of the auroral oval (as in the last 2 panels in Figure 5). When the IMF By component is nearly zero (center panel of Figure 7), the cusp aurora is centered on noon MLT. Finally, when IMF By component is positive (right hand panel), the cusp aurora emissions are located on the post-noon side of the auroral oval.

Figure 7 shows that the cusp aurora emissions during periods when the IMF is southward have the same local time dependence with IMF By as the cusp aurora during periods when the IMF is northward. Figure 8 shows how the anti-parallel neutral line model of reconnection may explain this local time dependence with IMF By. The three panels (again, adopted from Crooker, (1979)) correspond to the three panels in Figure 7 (however, the view perspective in Figure 7 is from the Earth and, in Figure 8, it is from the Sun).

In the left hand panel of Figure 8, there are two neutral lines originating from the northern and southern hemisphere cusps. These neutral lines trace the location where the southward and dawnward (−By) IMF is anti-parallel to the magnetospheric field lines at the magnetopause. Since the observations in Figure 7 are from June (northern hemisphere summer), the ecliptic plane is located near the northern hemisphere neutral line and the southern hemisphere neutral line is well below

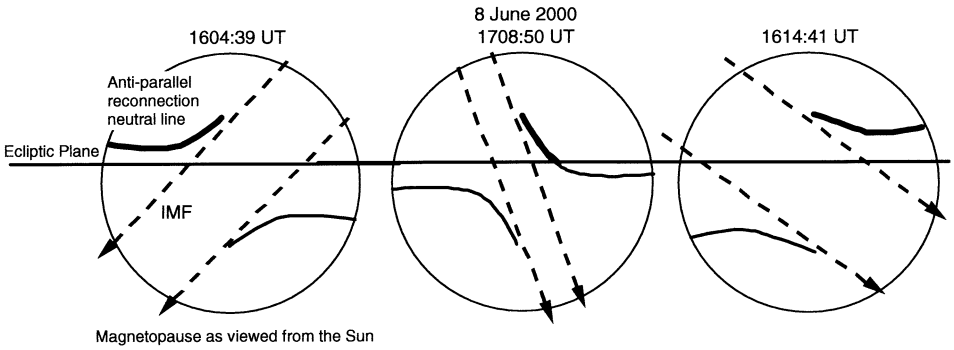

Figure 8. Anti-parallel reconnection neutral lines on the magnetopause for the three intervals in Figure 7. As the IMF By changes sign, the neutral line in the northern hemisphere switches position relative to the noon-midnight meridian. The IMAGE SI12 only observes precipitation from this neutral line (and not from the neutral line in the southern hemisphere). Thus, the anti-parallel neutral line model correctly predicts that the cusp will appear pre- (post-) noon when the IMF By component is negative (positive).

the ecliptic plane. Figure 6 shows that the opposite is true for the observations in Figure 5 from November (northern hemisphere winter).

In the middle panel of Figure 8, the IMF has a slight duskward (+By) component. In the anti-parallel neutral line model, the IMF By=0 condition is an inflection point where the neutral lines originate from the cusps follow the noon-midnight meridian to the equator and then follow the equator around to the flanks of the magnetopause. However, the slight positive By component (see the middle panel in Figure 7), causes this symmetry to be broken and the neutral lines split at the noon midnight meridian. The neutral line in the northern hemisphere is now on the duskside of the magnetopause while the neutral line in the southern hemisphere is on the dawnside magnetopause. Because the IMF Bz component dominates, the neutral line dips to lower latitudes than in either the left or right hand panels. The dip is significant enough to cause the neutral line in the northern hemisphere to be below the ecliptic.

In the right hand panel, the IMF has a significant duskside (+By) component and the neutral lines are once again at high latitudes and the one in the northern hemisphere is on the duskside of the magnetopause. For this time period, the By component is large enough such that the neutral line in the northern hemisphere is entirely above the ecliptic plane.

Figure 8 shows that the anti-parallel neutral line model correctly predicts that the cusp emissions will follow the IMF By component (with emissions on the dawnside for −By and on the duskside for +By) provided that the SI12 images proton precipitation exclusively from the northern hemisphere neutral line.

The changes in the reconnection acceleration in the presence magnetosheath flow combined with the characteristics of the SI12 imager provide an explanation for the inability to image emissions from the southern hemisphere neutral line.

Ions precipitating in the northern hemisphere cusp crossed the magnetopause either poleward of the reconnection neutral line in the northern hemisphere or equatorward of the neutral line in the southern hemisphere. In either case, ions are accelerated in the direction of the reconnected field line convection upon crossing the magnetopause. Ions that precipitate in the northern hemisphere ionosphere cross the magnetopause with nearly zero pitch angle. Thus, the change in velocity across the open magnetopause for the field-aligned ions is critical for determining their precipitation energy.

The reconnected magnetic field lines poleward of the neutral line in the northern hemisphere (above the equatorial plane) convect tailward, in the same direction as the magnetosheath flow. Field-aligned ions crossing the magnetopause poleward of this neutral line experience an acceleration that is nearly in the same direction as the magnetosheath flow. This acceleration is maximum for the ions crossing at or very near the neutral line, because the magnetic fields are most nearly anti-parallel in that location. For ions crossing equatorward of the neutral line in the southern hemisphere the same process occurs but the acceleration is nearly opposite the magnetosheath flow direction. The reconnected field lines propagating toward the north, away from this southern hemisphere neutral line must overcome the magnetosheath flow. Thus, the field-aligned ion flow will be lower for these ions than for the ones crossing the reconnection site poleward of the northern hemisphere neutral line.

The non-linear response of the SI12 imager to the energy of the precipitating protons accentuates the difference in the precipitating energy of the ions from the two neutral lines. The energy differences of the precipitating ions will cause the cusp aurora emissions to be significantly more intense pre-noon when compared to post-noon when the IMF has a negative B_y component (left hand panels of Figures 7 and 8). From this explanation of the cusp proton aurora, there are several predictions. First, the local time location of the observed emissions will be opposite in the two hemispheres since the neutral lines are located on opposite sides of the noon-midnight meridian. This prediction can only be truly verified by simultaneous observations of the cusp proton auroras in the two hemispheres. However, starting in about 2004, IMAGE will observe the southern hemisphere and should observe the opposite local time dependence with IMF By. Partial confirmation also comes from previous statistical studies using in situ data. Although not separated by IMF Bz component, Newell *et al.* (1989) demonstrated that the changes in the cusp location with IMF By are opposite in the southern hemisphere. Second, direct measurements of the cusp should show a significant energy (and possibly flux) difference between pre-noon and post-noon. While there has been no direct test of this prediction to date, there is some indirect evidence that there is indeed a difference between pre- and post-noon precipitation. Using a specific definition of cusp precipitation, the 'cusp' has been shown to move to pre-noon when the IMF By is negative and post-noon when the IMF By component is positive (e.g., Newell *et al.*, 1989). However, in the above interpretation, the cusp precipitation

occurs both pre- and post-noon and the difference is simply the highest energies of the precipitating ions on either side of noon. Thus, it remains to be shown that the definition of the cusp used by Newell and Meng (1988; 1992) and the observations in Figure 7 are consistent with one another. Additional indirect evidence comes from global MHD simulations. These simulations (Berchem *et al.*, this volume) show that, in the northern ionosphere, the velocities of the precipitating ions from the northern hemisphere neutral line are significantly higher than those from the southern hemisphere neutral line.

6. Summary of Cusp Aurora Observations

The above observations of the cusp aurora demonstrate that there is a distinct dynamic response of the cusp to changes in the IMF. When the IMF is northward, the cusp is fairly well localized as a spot at high latitude, poleward of the auroral oval. When the IMF By component is positive (negative), the spot is located at post- (pre-) noon magnetic local time. When the IMF turns southward, this spot moves equatorward and spreads out along the auroral oval. For southward IMF, the magnetic local time position of the cusp emissions has the same dependence on IMF By as that for northward IMF.

The IMAGE observations provide two unique perspectives of the cusp footpoint which have implications on the 'when' and 'where' of magnetic reconnection at the magnetopause. First, the IMAGE observations of continuous cusp precipitation show that, although the reconnection rate may vary, it is never zero. Whether the IMF is steady or the By, or Bz components are changing, reconnection continues at the magnetopause.

Second, the changes in the location of the cusp with IMF By and the localization of cusp precipitation provide important clues to the location of reconnection at the magnetopause. In this paper, the changes in the cusp footpoint with IMF By and Bz and the localization of the cusp footpoint when the IMF Bz component was positive were interpreted in terms of the anti-parallel reconnection model. These observations provide strong support for this model. However, the observations for southward IMF have not been shown to be incompatible with the component reconnection model. In the component or tilted neutral line model, the neutral line tilt direction and magnitude depend on IMF By in a similar manner as the location of the anti-parallel reconnection sites (see Figure 1). The two models differ only in the region around the subsolar point. Thus, it remains to be shown that the IMAGE observations of the cusp aurora favor one or the other neutral line model.

Finally, there is an apparent discrepancy between the interpretations of the proton aurora observed for northward IMF and the aurora observed for southward IMF that requires further consideration. Using Figures 5, 6, 7, and 8, it was argued that, for southward IMF, there is a significant reduction in the energy of the precipitating protons if they cross a neutral line that is convecting in a direction that is against the

prevailing flow direction in the magnetosheath. However, this condition is always true for the high latitude reconnection site (poleward of the cusp) for northward IMF. At this site, reconnected field lines are convected sunward, in the direction opposite the magnetosheath flow. Applying the southward IMF interpretation to northward IMF conditions suggests that there should be no cusp aurora observed for high latitude reconnection during northward IMF. The apparent discrepancy may be explained by unusually low flow velocities in the magnetosheath adjacent to the high latitude magnetopause during northward IMF. These flow velocities are certainly sub-Alfvenic (Fuselier *et al.*, 2000), and may be comparable to flow velocities observed in the subsolar region (Onsager *et al.*, 2001; Fuselier *et al.*, 2002c). These low flow velocities suggest that the energy gained by ions crossing the high latitude reconnection site is not affected by magnetosheath flow in the vicinity of the region poleward of the cusp.

7. Ionospheric Outflow from the Dayside Auroral Oval and the Cusp

The above observations show that the FUV imagers on the IMAGE spacecraft can readily image the cusp (at least when the solar wind dynamic pressure is high). This ability to image the cusp provides an opportunity to resolve a long-standing problem in magnetospheric physics that is related to the dynamic response of the auroral oval to changes in the solar wind.

Since the discovery of ions of ionospheric origin in the Earth's magnetosphere (Shelley *et al.*, 1972), the origin of these ions has been a topic of considerable study. Studies of in situ observations at a wide range of altitudes have concluded that these ionospheric ions originate in the auroral zone at high latitudes. Statistical studies of large databases indicate that ionospheric outflow depends on season, solar cycle, and magnetospheric activity (e.g., Yau *et al.*, 1985; Collin *et al.*, 1998; Øieroset *et al.*, 1999). These studies demonstrate that there is a strong correlation between ion outflow and the auroral zone. Because these studies use large databases of single point measurements; however, they do not provide information on what part of the auroral oval is actively producing ionospheric outflow at any instant time. Thus, two competing models for ionospheric outflow have been developed. Moore *et al.* (1985) suggested that an intense, localized ionospheric outflow from the cusp provides the ionospheric ions for the magnetosphere. In contrast, Shelley *et al.* (1985) suggested that the outflow region was diffuse and extending over the entire auroral oval. In many ways, the lingering controversies concerning ion outflow parallel those of magnetic reconnection. Despite over 30 years of in situ observations, there are still issues concerning the 'when' and the 'where' of ion outflow.

The Low Energy Neutral Atom (LENA) imager (Moore *et al.*, 2000) detects neutrals created by charge exchange of ionospheric ions with the Earth's upper atmosphere and geocorona. It was designed to provide images of the ionospheric

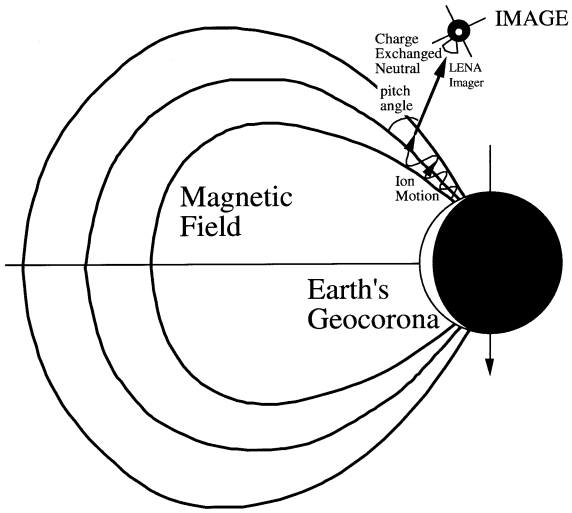

Figure 9. Illustration of charge exchange of ionospheric outflow. Ions from the auroral oval spiral along the Earth's magnetic field and charge exchange with the neutral atmosphere and geocorona. Upon charge exchange, the resulting neutral propagates in a straight line. By tracing back along the arrival direction of the neutral, the charge exchange altitude and the pitch angle of the ionospheric ion is determined.

outflow on timescales commensurate with magnetospheric activity (i.e., many images over a typical magnetospheric sub-storm timescale of about 1 hour) with the intention of resolving the lingering issues concerning when and where ion outflow is occurring. While it has the ability to distinguish mass, this review focuses on Hydrogen outflow.

Figure 9 is a schematic diagram of an ionospheric ion that follows the magnetic field to a certain altitude and, upon charge exchange, becomes a neutral that propagates in a straight line to the spacecraft. The direction of travel of the neutral (in three dimensions) is determined by the pitch angle relative to the magnetic field and the phase angle in its motion around the magnetic field when the ion charge exchanges. Two features are evident from Figure 9. First, the pitch angle of the ionospheric ion is preserved in the charge exchange process and second, the direction of arrival is related to the charge exchange altitude (given that the ionospheric ion originated in the northern hemisphere). Thus, the LENA imager obtains a snapshot of the ionospheric outflow convolved with the geocoronal hydrogen distribution and the pitch angle viewed from a given spacecraft location. If ionospheric ion fluxes were independent of pitch angle, then the location of the spacecraft would not be important. However, the pitch angle distributions of ionospheric ion outflows are not isotropic (e.g., Peterson *et al.*, 1992) and spacecraft position plays a critical role in the interpretation of the LENA images.

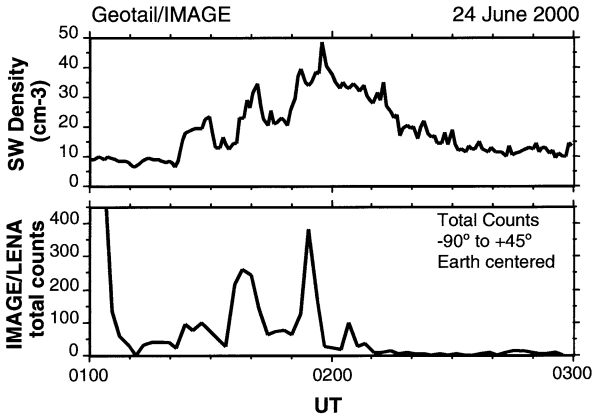

Figure 10. (Top panel) solar wind density (time convected to the ionosphere) (bottom panel) Countrate from the Earth direction in the LENA imager. The peaks in the solar wind density correlate well with peaks in the ion outflow rate observed by LENA.

8. Observations on 24 June 2000

Figure 10 shows two hours of solar wind and LENA data from 24 June 2000. The solar wind data have been convected in time to account for the time required for a solar wind disturbance to arrive in the ionosphere (1–2 minutes from the Geotail spacecraft in the solar wind) and the time for an ionospheric ion to propagate to the IMAGE spacecraft (an additional 3 minutes, assuming ∼50 eV hydrogen). During the two-hour period in Figure 10, the IMAGE spacecraft changed position from nearly the dusk terminator at low altitude (∼1 R_E) to over the north pole at relatively high altitude (∼4 R_E). As the spacecraft exited the radiation belts and entered the polar cap (from 0100 to 0110 UT), the LENA integrated count rate from the Earth direction (integrated over a 90 × 135 area centered approximately on the Earth direction) initially decreased. However, over the period from 0110 UT to 0210 UT, there are five distinct peaks in the LENA countrate. These peaks are associated with distinct changes in the solar wind density (top panel of Figure 10).

Figure 10 shows that there is a direct association between changes in the solar wind and changes in the ionospheric outflow. Furthermore, it shows that the ionospheric outflow is 'prompt' in response to changes in the solar wind. The time delay between the arrival of a solar wind disturbance in the ionosphere (assuming propagation through the magnetosheath, across the magnetopause, and along the magnetospheric field lines to the ionosphere) and the arrival of neutrals at the spacecraft can be accounted for entirely by the ∼3 minute propagation time for a ∼50 eV neutral hydrogen atom created by charge exchange of an ionospheric hydrogen ion with the Earth's geocorona (i.e., following a path similar to that illustrated in Figure 9). Thus, there is no delay in the ionosphere between the arrival time of the solar wind disturbance and any heating that starts the ion outflow process (see also, Moore *et al.*, 1999; 2001; Fuselier *et al.*, 2001, 2002b).

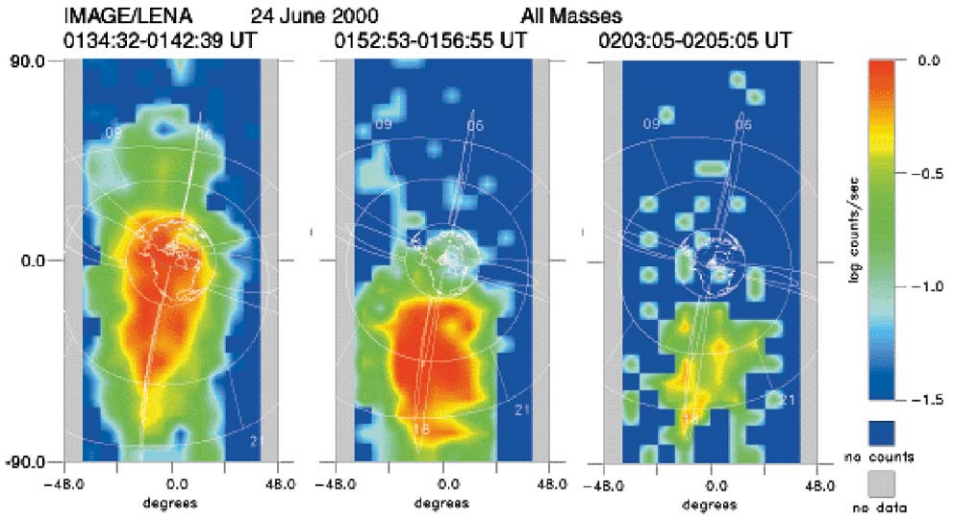

Figure 11. Images of three of the ionospheric outflow bursts in Figure 10. In the first image, the outflow is centered somewhat on the Earth direction. In subsequent images, the peak outflow occurs off the Earth direction.

In situ observations have shown that ion outflow probably never ceases. For the most part, they have failed to address the problem of time delay between an external event that initiates ion outflow and the outflow itself. Figure 10 shows that the time delay is zero. Thus, concerning when outflow occurs, IMAGE has been able to demonstrate that outflow is a prompt process initiated by, for example, changes in the solar wind density.

The question of where ion outflow occurs is much more difficult to address. Figure 11 shows the LENA images of three of the outflow bursts in Figure 10. In each panel, the view is from the IMAGE spacecraft (located on the duskside of the magnetosphere) with the Earth in the center. Magnetic field lines are shown at L shells of 3 and 5. For all three panels, the neutral flux is mainly seen on the duskside and well off the direction of the Earth. Considering Figure 9, the duskside neutral flux coming from off the Earth direction comes from duskside ionospheric outflow that has charge exchanged at fairly high altitude and propagated to the spacecraft. From the spacecraft vantage point on the duskside, neutrals from outflow from the dawnside, noon, or midnight sectors would either appear from the Earth direction if the charge exchange altitude is low or from the dawnside, noon, or midnight directions for high altitude charge exchange.

Figure 12 shows the ray tracing of one of these duskside magnetic field lines. In the lower left hand panel, the IMAGE FUV/Wideband Imaging Camera (WIC) image of the auroral oval is shown. This imager detects FUV emissions in the wavelength range from 140 to 180 nm produced by precipitating electrons (primarily) and precipitating protons (when their flux is much higher than the electron flux, in regions such as the cusp). The X on the duskside peak in the auroral emissions

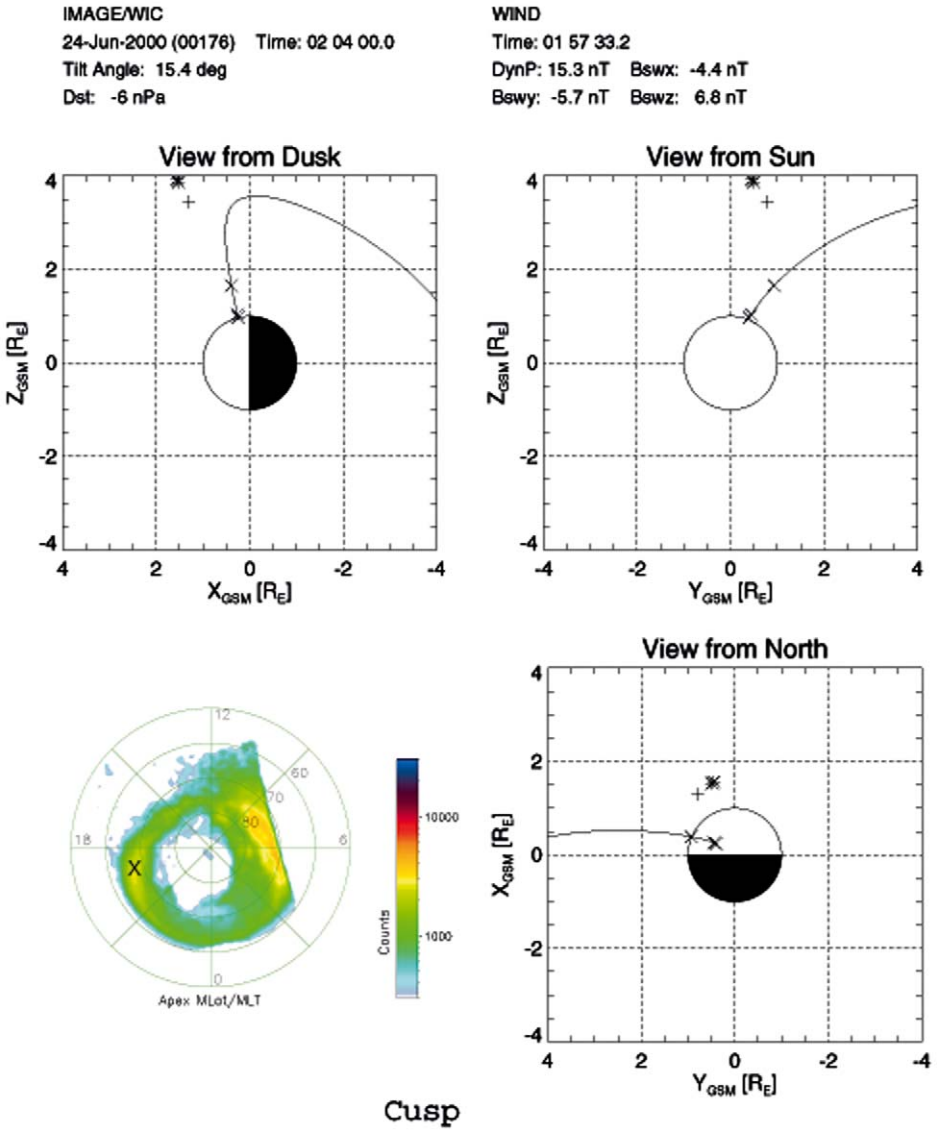

Figure 12. Mapping of the duskside auroral field line where the emissions are greatest. The upper left, upper right, and lower right hand panels show three perspectives of the field line mapped from the peak in the UV aurora image on the duskside (marked by the 'x' in the image in the lower left hand panel). The three marks along the field line show the origin of neutrals produced by charge exchange of ion outflow if the charge exchange occurs at 500, 1000, and 6000 km. The asterisk shows the location of the IMAGE spacecraft. The ions at the three altitudes where charge exchange occurs would need to have specific pitch angles in order to reach the spacecraft.

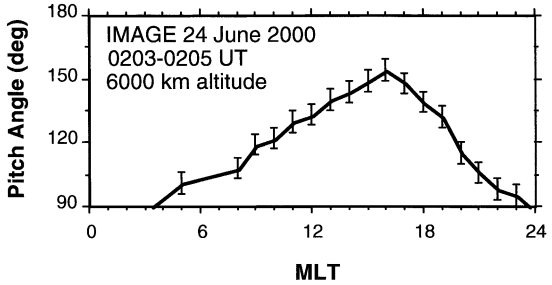

Figure 13. Pitch angle of the ionospheric ions that can be observed by LENA as a function of MLT for the ionospheric ion burst in the right hand panel of Figure 10. Peak neutral flux comes from charge exchange of ions with ∼120°–140° at 18 magnetic local time.

shows the origin of the magnetic field line traced out into the magnetosphere in the other three panels. This field line crosses the equator somewhere near the dusk terminator. To be detected by the LENA imager, ions must propagate along the field line, charge exchange at some altitude (for example 6000 km, shown by an x along the field line) and propagate in a straight line to the IMAGE spacecraft location after charge exchange. Given the magnetic field direction, the direction of arrival of the neutral created by this charge exchange process indicates the altitude of the charge exchange event. Furthermore, by knowing the direction of arrival, the pitch angle of the ionospheric ion is known. For example, in Figure 12, an ion from the peak in the auroral emissions at ∼1900 MLT on the auroral oval that charge exchanges at 6000 km altitude would have a pitch angle of 133°. Since the magnetic field is directed into the northern ionosphere, this angle represents outflowing ionospheric ions with an angle of ∼45° relative to the magnetic field. Neutrals produced by charge exchange of ionospheric ion outflow that had pitch angles larger or smaller than 130°–140° would not be detected by the LENA imager because their trajectories would not intersect the IMAGE spacecraft.

Comparing this ray tracing result with the neutral flux images in Figure 11, it is clear that IMAGE is observing outflow primarily from the duskside ionosphere that had fairly large pitch angles relative to the magnetic field. Thus, one conclusion obtained from this image is that intense ionospheric outflow occurs in regions of the auroral zone where there are significant auroral emissions. However, Figure 12 shows that there are also significant emissions on the dawnside of the auroral oval. More importantly, the spot located at about 85° latitude and 11 MLT in the auroral image shows the location of the cusp (this image was taken during a northward IMF solar wind interval). The LENA imager failed to detect significant ionospheric outflow from these two regions of relatively intense auroral emissions.

The failure to detect ionospheric outflow from these regions may be explained by considering the range of pitch angles seen from the IMAGE spacecraft vantage point. By tracing individual magnetic field lines from the auroral oval at all local times in Figure 12 and assuming a ∼6000 km charge exchange altitude, a map

is developed of the pitch angles seen from the IMAGE spacecraft location as a function of local time for the outflow. Figure 13 shows the result of this map for the outflow burst in the left hand panel of Figure 10. This map has some significant features. First, the pitch angle range for outflow between 0 and 3 MLT is less than 90°. Thus, no outflow from this region can be imaged because the LENA imager is observes pitch angles of ions that are propagating toward the ionosphere and not ions that are propagating away from the ionosphere. Second, at the cusp location (∼11 MLT), LENA is observing large pitch angles, similar to the pitch angles observed at 18 MLT (where the peak in the neutral flux is coming from in Figure 11). At lower charge exchange altitudes, the pitch angle observed by LENA does not change drastically. Thus, Figure 12 shows that ionospheric outflow from the cusp should have been imaged if there was significant flux at large pitch angles.

In situ measurements have shown that this is not the case. Cusp ionospheric outflow is in the form of field-aligned beams (i.e., ion distributions that have significant flux over a narrow range of pitch angles that are centered on the magnetic field direction). In contrast, outflow from the rest of the auroral oval can be in the form of beams or conics (i.e., ion distributions with significant flux at a narrow range of pitch angles that are highly oblique to the magnetic field). In fact, these conic distributions have peak flux between 110° and 140°, in good agreement with the ∼130° pitch angles seen from the duskside outflow in Figure 11. Unfortunately, these differences in the ionospheric outflow make it difficult to make a simultaneous image of the outflow from the auroral oval and the cusp at the same time. Such an image is possible, but it requires a rather unique spacecraft location that can view small pitch angles along the cusp direction and large pitch angles from the rest of the auroral oval. Thus, even with global imaging of the ionospheric outflow, it will be difficult to resolve the controversy surrounding where ionospheric outflow occurs. IMAGE can only demonstrate that, provided the spacecraft location allows imaging of the correct range of pitch angles, the most intense ionospheric outflow occurs in the region where the auroral emissions are also most intense. Further analysis of other events is necessary to determine if IMAGE is ever in the proper location to make simultaneous observations of outflow from the cusp and the rest of the auroral oval.

In summary, the LENA imager is able to image ionospheric outflow over long periods of time (∼1 hour). This imaging demonstrates that ionospheric outflow is prompt in response to changes in the solar wind and occurs in regions where the auroral emissions are most intense. Finally, the pitch angle of the ionospheric outflow plays an important role in determining the neutral flux observed by LENA.

9. Summary and Conclusions

The IMAGE spacecraft has provided new perspectives on the coupling of the dayside aurora with the Earth's magnetosphere. Examples in the paper show that the

magnetospheric cusps are coupled to the Earth's magnetopause and respond to dynamic changes in the solar wind. In particular, one manifestation of magnetic reconnection at the magnetopause is the precipitation of magnetosheath protons into the ionosphere. Images of the Doppler-shifted Lyman Alpha produced by the precipitation of magnetosheath protons (after they are converted to Hydrogen by collisions in the upper atmosphere) show that the cusp footpoint is continuously present, even when the IMF rotates from north to south. This result demonstrates that reconnection is a continuous process and that the reconnection rate does not decrease to zero for any extended period of time. The location of the cusp footpoint depends on IMF By and Bz. When the IMF is northward (+Bz), the cusp footpoint is a highly localized spot located poleward of the auroral oval. Field lines from this spot map to a narrow region on the magnetopause poleward of the cusp where the magnetosheath field lines draped against the magnetopause are anti-parallel to the magnetospheric magnetic field lines. The spot moves with IMF By and is located pre- (post-) noon MLT when By is negative (positive). When the IMF turns southward, the cusp footpoint moves equatorward and spreads out along the auroral oval. The cusp footpoint has the same local time dependence with IMF By as that for northward IMF. Once again, this local time dependence is predicted from the anti-parallel reconnection model. However, the tilted neutral line (component reconnection) model has not been ruled out by these observations.

The cusp and the rest of the auroral oval is also a region of ion outflow. Ion outflow responds promptly to changes in the solar wind. In particular, bursts of ion outflow are correlated with increases in the solar wind density. Although the LENA imager monitors ion outflow over long periods of time (hours), the pitch angle characteristics of the outflow limit the interpretation of the outflow images. These characteristics suggest that special spacecraft locations will be required to observe simultaneously ion outflow from the cusp and from the rest of the auroral oval.

Although additional studies of the IMAGE data (including observations from other imagers on the spacecraft) likely will reveal new aspects of the dayside aurora and its dynamic relationship to the solar wind, the results discussed in this paper indicate that this aspect of IMAGE science has been highly successful.

Acknowledgements

The success of the IMAGE mission is a tribute to the many dedicated scientists and engineers that have worked and continue to work on the project. The PI for the mission is Dr. J. Burch. Solar wind observations in this paper are from the NASA CDAWeb.

References

Burch, J.L.: 1973, 'Rate of erosion of dayside magnetic flux based on a quantitative study of polar cusp latitude on the interplanetary field', *Radio Sci.* **8**, 955.

Burch, J.L., Menietti, J.D. and Barfield, J.N.: 1986, 'DE-1 Observations of solar wind-magnetospheric coupling processes in the polar cusp', in *Solar Wind-Magnetosphere Coupling*, edited by Kamide, Y. and Slavin, J.A., p. 441, Terra Sci., Tokyo.

Candidi, M., Mastranntonio, G., Orsini, S. and Meng, C.-I.: 1989, 'Evidence for the influence of the interplanetary magnetic field azimuthal component on the polar cusp configuration', *J. Geophys. Res.* **94**, 13,585.

Carbary, J.F. and Meng, C.-I.: 1988, Correlation of cusp width with AE(12) and Bz, *Planet. Space Sci.* **36**, 157.

Collin, H.L., Peterson, W.K., Lennartsson, O.W., Drake, J.F.: 1998, 'The seasonal variation of auroral ion beams', *Geophys. Res. Lett.* **25**, 4071.

Crooker, N.U.: 1979, 'Dayside merging and cusp geometry', *J. Geophys. Res.* **84**, 951.

Frank, L.A.: 1971, 'Plasmas in the Earth's polar magnetosphere', *J. Geophys. Res.* **76**, 5202.

Frey, H.U., Mende, S.B., Immel, T.J., Fuselier, S.A., Claflin, E.S., Gérard, J.-C. and Hubert, B.: 2002, 'Proton aurora in the cusp', *J. Geophys. Res.* **107**(A7), 1091, DOI 10.1029/2001JA900161.

Fuselier, S.A., Anderson, B.J. and Onsager, T.G.: 1997, 'Electron and ion signatures of field line topology at the low-shear magnetopause', *J. Geophys. Res.* **102**, 4847.

Fuselier, S.A., Ghielmetti, A.G., Moore, T.E., Collier, M.R., Quinn, J.M., Wilson, G.R., Wurz, P., Mende, S.B., Frey, H.U., Jamar, C., Gerard, J.-C. and Burch, J.L.: 2001, 'Ion outflow observed by IMAGE: Implications for source regions and heating mechanisms', *Geophys. Res. Lett.* **28**, 1163.

Fuselier, S.A., Frey, H.U., Trattner, K.J., Mende, S.B. and Burch, J.L.: 2002a, 'Cusp auroral dependence on IMF Bz', *J. Geophys. Res.* **107**(A7), 1111, DOI 10.1029/2001JA900165.

Fuselier, S.A., Collin, H.L., Ghielmetti, A.G., Claflin, E.S., Moore, T.E., Collier, M.R., Frey, H. and Mende, S.B.: 2002b, 'Localized ion outflow in response to a solar wind pressure pulse', *J. Geophys. Res.* **107**(A7), 1203, DOI 10.1029/2001JA000297.

Fuselier, S.A., Waite, Jr., J.H., Avanov, L.A., Smirnov, V.M., Vaisberg, O.L., Siscoe, G.L. and Russell, C.T.: 2002c, 'Characteristics of magnetosheath plasma in the vicinity of the high altitude cusp', *Planet. Space Sci.* **50**, 559–566.

Gérard, J.-C., Hubert, B., Meurant, M., Shematovitch, V.I., Bisikalo, D.V., Frey, H., Mende, S., Gladstone, G.R. and Carlson, C.W.: 2001, 'Observation of the proton aurora with IMAGE FUV imager and simultaneous ion flux in situ measurements', *J. Geophys. Res.* **106**, 28,939.

Gosling, J.T. and Robson: 1985, 'Ion reflection, gyration, and dissipation at supercritical shocks', in *Collisionless Shocks in the Heliosphere: Reviews of Current Ressearch, Geohpys. Monogr. Ser., vol 35*, edited by B.T. Tsurutani, B.T. and Stone, R.G., p. 141, AGU Washington, D.C.

Gosling, J.T., Thomsen, M.F., Bame, S.J., Elphic, R.C. and Russell, C.T.: 1990, 'Plasma flow reversals at the dayside magnetopause and the origin of asymmetric polar cap convection', *J. Geophys. Res.* **95**, 8073.

Heikkila, W.J. and Winningham, J.D.: 1971, 'Penetration of magnetosheath plasma to low altitudes through the dayside magnetospheric cusps', *J. Geophys. Res.* **76**, 883.

Mende, S.B., *et al.*, 'Far ultraviolet imaging from the IMAGE spacecraft', *Space Sci. Rev.* **91**, 287.

Mende, S.B., Frey, H.U., Lampton, M., Gerard, J.-C., Hubert, B., Fuselier, S., Spann, J., Gladstone, R. and Burch, J.L.: 2001, 'Global observations of proton and electron auroras in a substorm', *Geophys. Res. Lett.* **28**, 1139.

Milan, S.E., Lester, M., Cowley, S.W.H. and Brittnacher, M.: 2000, 'Dayside convection and auroral morphology during an interval of northward interplanetary magnetic field', *Ann. Geophysicae* **18**, 436.

Moore, T.E., Chappell, C.R., Lockwood, M. and Waite, Jr., J.H.: 1985, 'Superthermal ion signatures of auroral acceleration processes', *J. Geophys. Res.* **90**, 1611.

Moore, T.E. *et al.*: 1999, 'Ionospheric mass ejection in response to a CME', *Geophys. Res. Lett.* **26**, 2339.

Moore, T.E. *et al.*: 2000, 'The low-energy neutral atom imager for IMAGE', in *The IMAGE Mission*, ed. Burch, J.L., Kluwer Academic Publishers, Dordrecht, p. 155–195.

Moore, T.E. *et al.*: 2001, 'Low energy neutral atoms in the magnetosphere', *Geophys. Res. Lett.* **28**, 1143.

Newell, P.T., and Meng, C.-I.: 1988, 'The cusp and cleft/LLBL: Low latitude identification and statistical local time variation', *J. Geophys. Res.* **93**, 14,549.

Newell, P.T. and Meng, C.-I.: 1992, 'Mapping the dayside ionosphere to the magnetosphere according to particle precipitation characteristics', *Geophys. Res. Lett.* **19**, 609.

Newell, P.T. and Sibeck, D.G.: 1993, 'By fluctuations in the magnetosheath and azimuthal flow velocity transients in the dayside ionosphere', *Geophys. Res. Lett.* **20**, 1719.

Newell, P.T., Meng, C.-I., Sibeck, D.G. and Lepping, R.: 1989, 'Some low-altitude cusp dependencies on the interplanetary magnetic field', *J. Geophys. Res.* **94**, 8921.

Øieroset M., Yamauchi, M., Liszka, L. and Hultqvist, B.: 1999, 'Energetic ion outflow from the dayside ionosphere: Categorization, classification and statistical study', *J. Geophys. Res.* **104**, 24,915.

Onsager, T.G., Kletzing, C.A., Austin, J.B. and MacKiernan, H.: 1993, 'Model of magnetosheath plasma in the magnetosphere: Cusp and mantle particles at low altitudes', *Geophys. Res. Lett.* **20**, 479.

Peterson, W.K., Collin, H.L., Doherty, M.F. and Bjorklund, C.M.: 1992, 'O^+ and He^+ restricted and extended (b-modal) ion conic distributions', *Geophys. Res. Lett.* **19**, 1439.

Phan, T.D. *et al.*: 2000, 'Extended magnetic reconnection at the Earth's magnetopause from detection of by-directional jets', *Nature* **404**, 848.

Reiff, P.H., Hill, T.W. and Burch, J.L.: 1977, 'Solar wind plasma injection at the dayside magnetospheric cusp', *J. Geophys. Res.* **82**, 479.

Rosenbauer, H., Gruenwaldt, H., Montgomery, M.D., Paschmann, G. and Sckopke, N.: 1975, 'HEOS 2 plasma observations in the distant polar magnetosphere: the plasma mantle', *J. Geophys. Res.* **80**, 2723.

Russell, C.T., Chappell, C.R., Montgomery, M.D., Neugebauer, M. and Scarf, F.L.: 1971, 'Ogo 5 observations of the polar cusp on November 1, 1968', *J. Geophys. Res.* **76**, 6743.

Shelley, E.G.: 1985, 'Circulation of energetic ions of terrestrial origin in the magnetosphere', *Adv. Space Res.* **5**, 401.

Shelley, E.G., Johnson, R.G. and Sharp, R.D.: 1972, 'Satellite observations of energetic heavy ions during a geomagnetic storm', *J. Geophys. Res.* **77**, 6104.

Smith, M.F. and Lockwood, M.: 1990, 'The pulsating cusp', *Geophys. Res. Lett.* **17**, 1069.

Sonnerup, B.U.: 1974,'Ö, Magnetopause reconnection rate', *J. Geophys. Res.* **79**, 1546.

Sonnerup, B.U., Paschmann, Ö.G., Papamastorakis, I., Sckopke, N., Haerendel, G., Bame, S.J., Asbridge, J.R., Gosling, J.T. and Russell, C.T.: 1981, 'Evidence for magnetic field reconnection at the Earth's magnetopause', *J. Geophys. Res.* **86**, 10,049.

Tsyganenko, N.A.: 1995, 'Modeling the Earth's magnetospheric magnetic field confined within a realistic magnetopause', *J. Geophys. Res.* **100**, 5599.

Wing, S., Newell, P.T. and Ruohoniemi, J.M.: 2001, 'Double cusp: Model prediction and observational verification', *J. Geophys. Res.* **106**, 25,571.

Woch J. and Lundin, R.: 1992, 'Magnetosheath plasma precipitation in the polar cusp and its control by the interplanetary magnetic field', *J. Geophys. Res.* **97**, 1421.

Yau, A.W., Beckwith, P.H., Peterson, W.K. and Shelley, E.G.: 1985, 'Long-term (solar cycle) and seasonal variations of upflowing ionospheric ion events at DE 1 altitudes', *J. Geophys. Res.* **90**, 6395.

Zhou, X.W., Russell, C.T., G.Le, Fuselier, S.A. and Scudder, J.D.: 2000, 'Solar wind control of the polar cusp at high latitude', *J. Geophys. Res.* **105**, 245.